

This article was downloaded by:

On: 23 January 2011

Access details: *Access Details: Free Access*

Publisher *Taylor & Francis*

Informa Ltd Registered in England and Wales Registered Number: 1072954 Registered office: Mortimer House, 37-41 Mortimer Street, London W1T 3JH, UK



## Journal of Coordination Chemistry

Publication details, including instructions for authors and subscription information:

<http://www.informaworld.com/smpp/title~content=t713455674>

### Synthesis, spectroscopy and electrochemical study of cobalt(III) $N_2O_2$ Schiff-base complexes

Ali Hossein Kianfar<sup>a</sup>; Solmaz Zargari<sup>b</sup>

<sup>a</sup> Department of Chemistry, Yasuj University, Yasuj, Iran <sup>b</sup> Department of Chemistry, Kurdistan University, Sanandaj, Iran

First published on: 31 July 2007

**To cite this Article** Kianfar, Ali Hossein and Zargari, Solmaz(2008) 'Synthesis, spectroscopy and electrochemical study of cobalt(III)  $N_2O_2$  Schiff-base complexes', *Journal of Coordination Chemistry*, 61: 3, 341 – 352, First published on: 31 July 2007 (iFirst)

**To link to this Article:** DOI: 10.1080/00958970701329217

**URL:** <http://dx.doi.org/10.1080/00958970701329217>

PLEASE SCROLL DOWN FOR ARTICLE

Full terms and conditions of use: <http://www.informaworld.com/terms-and-conditions-of-access.pdf>

This article may be used for research, teaching and private study purposes. Any substantial or systematic reproduction, re-distribution, re-selling, loan or sub-licensing, systematic supply or distribution in any form to anyone is expressly forbidden.

The publisher does not give any warranty express or implied or make any representation that the contents will be complete or accurate or up to date. The accuracy of any instructions, formulae and drug doses should be independently verified with primary sources. The publisher shall not be liable for any loss, actions, claims, proceedings, demand or costs or damages whatsoever or howsoever caused arising directly or indirectly in connection with or arising out of the use of this material.

## Synthesis, spectroscopy and electrochemical study of cobalt(III) N<sub>2</sub>O<sub>2</sub> Schiff-base complexes

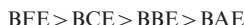
ALI HOSSEIN KIANFAR\*<sup>†</sup> and SOLMAZ ZARGARI<sup>‡</sup>

<sup>†</sup>Department of Chemistry, Yasuj University, Yasuj, Iran

<sup>‡</sup>Department of Chemistry, Kurdistan University, Sanandaj, Iran

(Received 3 December 2006; in final form 5 February 2007)

The complexes [Co(Chel)(PBU<sub>3</sub>)ClO<sub>4</sub>·H<sub>2</sub>O [Chel = BFE (*bis*(1,1,1-trifluoroacetylaceton) ethylenediimine) and BCE (*bis*(3-chloroacetylaceton)ethylenediimine)] and [Co(Chel)(PPh<sub>3</sub>)ClO<sub>4</sub>·H<sub>2</sub>O, (Chel = BBE = *bis*(benzoylaceton)ethylenediimine and BFE), were synthesized and characterized. The spectroscopic and electrochemical properties of cobalt(III) derivatives of BAE (*bis*(acetylaceton)ethylenediimine) and related ligands have also been investigated. Electronic spectroscopic data indicate that the absorption between 600 and 760 nm in Co(III) BAE complexes is related to the lowest d–d transition. Axial ligands affect this transition and the reduction potential of Co(III) to Co(II) through  $\sigma$ -interaction with the dz<sup>2</sup> orbital. The  $\pi$  acceptor property of Schiff-base ligands increases in the order:



**Keywords:** Phosphine; Cobalt; Spectroscopy; Schiff base; Electrochemistry

### 1. Introduction

Transition metal complexes with tetradentate Schiff-base ligands have been extensively investigated as catalysts for oxidation of organic compounds and electrochemical reductions [1–4]. Schiff-base complexes have also been used as catalytically active compounds to develop surface-modified electrodes as sensors [5, 6]. Cyclic voltammetry has been useful to investigate the mechanisms of catalysis and structure-reactivity relationships by Schiff-base complexes [2, 4, 7].

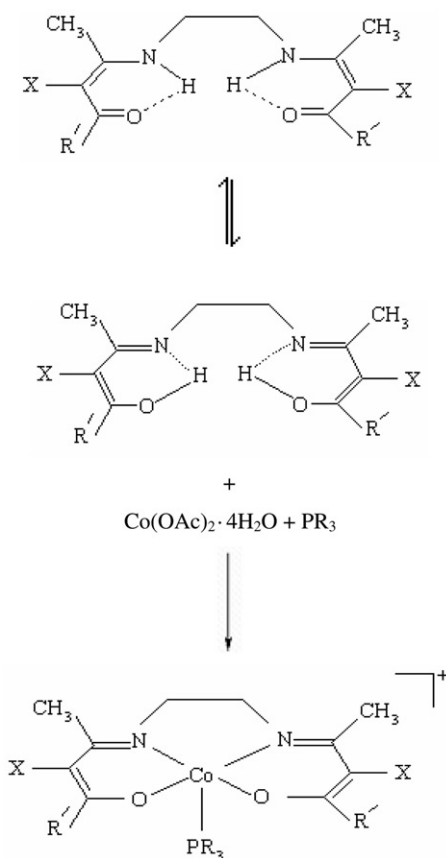
The electrochemical properties of Co(III) Schiff bases have been extensively studied [8–14]. In continuation of our studies on spectroscopy and electrochemistry of Co(III) Schiff-base complexes [15, 16], we report the synthesis and spectroscopic characterization of [Co(BBE)(PPh<sub>3</sub>)ClO<sub>4</sub>·H<sub>2</sub>O, and [Co(BFE)(PR<sub>3</sub>)ClO<sub>4</sub>·H<sub>2</sub>O, where R = Ph, Bu and [Co(BCE)(PBU<sub>3</sub>)ClO<sub>4</sub>·H<sub>2</sub>O. We have also studied the electronic spectra and the

\*Corresponding author. Tel.: +98-741-2223048. Fax: +98-741-2223048. Email: asarvestani@yahoo.com

electrochemical behavior of a series of Co(III) BAE complexes with the goal of evaluating the effect of axial ligand and equatorial substitutions (figure 1).

## 2. Experimental

All of the scanning UV-vis spectra were recorded by a JASCO V-530 spectrophotometer from 190 to 900 nm. The NMR spectra were recorded on a Bruker Avance



Chel	R'	R	X
BAE	CH <sub>3</sub>	Ph, Bu	H
BBE	Ph	Ph, Bu	H
BFE	CF <sub>3</sub>	Ph, Bu	H
BCE	CH <sub>3</sub>	Bu	Cl

Figure 1. The structure of Schiff bases and  $[\text{Co}(\text{Chel})(\text{PR}_3)]\text{ClO}_4 \cdot \text{H}_2\text{O}$  complexes.

DPX 250 MHz spectrometer; IR spectra were recorded by a Perkin Elmer 781 infrared spectrophotometer from 400 to 4000  $\text{cm}^{-1}$ . Elemental analyses were performed by using a Heraeus CHN-O-RAPID elemental analyzer.

## 2.1. Materials

Ethylenediamine, cobalt(II)acetate tetrahydrate, tributylphosphine, triphenylphosphine, acetylacetone, benzoylacetone, 3-chloroacetylacetone 1,1,1-trifluoroacetylacetone, tetrabutylammonium perchlorate, dimethylformamide, acetonitrile, methanol, ethanol, chloroform and sodium perchlorate monohydrate were purchased from Merck, Aldrich and Fluka.

## 2.2. Synthesis of the Schiff-base ligands and their Co(III) complexes

The ligands *bis*(acetylacetone)ethylenediimine (BAE), *bis*(benzoylacetone)ethylene diimine (BBE), *bis*(3-chloroacetylacetone)ethylenediimine (BCE) and *bis*(1,1,1-trifluoroacetylacetone)ethylenediimine (BFE), were prepared according to the literature [14, 17].  $\text{Co}(\text{BAE})(\text{PR}_3)\text{ClO}_4 \cdot \text{H}_2\text{O}$  (R = Ph, Bu) and  $[\text{Co}(\text{BBE})(\text{PBu}_3)]\text{ClO}_4 \cdot \text{H}_2\text{O}$  were prepared as described previously [18, 19]. The general procedure for synthesis of  $[\text{Co}(\text{BBE})(\text{PPh}_3)]\text{ClO}_4 \cdot \text{H}_2\text{O}$ ,  $[\text{Co}(\text{BCE})(\text{PBu}_3)]\text{ClO}_4 \cdot \text{H}_2\text{O}$  and  $[\text{Co}(\text{BFE})(\text{PR}_3)]\text{ClO}_4 \cdot \text{H}_2\text{O}$ , (where R = Bu and Ph) follow. To a refluxing solution of Schiff-base ligand (1.0 mmol), in methanol (100  $\text{cm}^3$ ),  $\text{Co}(\text{CH}_3\text{COO})_2 \cdot 4\text{H}_2\text{O}$  (1.0 mmol) and  $\text{PR}_3$  (1.0 mmol) were added. The formed Co(II) complex was oxidized by blowing air into the solution for two hours, and then the solution was filtered. To the filtrate, an appropriate amount of sodium perchlorate was added. Green precipitates formed after addition of water. The precipitates were washed with water and dried in vacuum at  $T = 343 \text{ K}$ .

Elemental analysis for  $[\text{Co}(\text{BBE})(\text{PPh}_3)]\text{ClO}_4 \cdot \text{H}_2\text{O}$ ,  $\text{C}_{40}\text{H}_{39}\text{CoClN}_2\text{O}_7\text{P}$  (785.06), yield: 75%. Calcd: C 61.19, H 5.01, N 3.57. Exp.: C 61.81, H 5.05, N 3.63.  $^1\text{H}$  NMR (250 MHz,  $\text{DMSO-d}_6$ , room temperature, TMS):  $\delta = 2.40$  ppm (s, 6H,  $\text{CH}_3$ ), 3.44 ppm (s, 4H,  $\text{CH}_2\text{CH}_2$ ), 5.45 ppm (s, 2H, CH), 7.21–8.22 ppm (m, 25H, Ar).

$[\text{Co}(\text{BFE})(\text{PBu}_3)]\text{ClO}_4 \cdot \text{H}_2\text{O}$ ,  $\text{C}_{24}\text{H}_{41}\text{CoClF}_6\text{N}_2\text{O}_7\text{P}$  (708.91), yield: 80%. Calcd: C 40.66, H 5.83, N 3.95. Exp.: C 41.01, H 5.81, N 4.01.  $^1\text{H}$  NMR (250 MHz,  $\text{DMSO-d}_6$ , room temperature, TMS):  $\delta = 0.57$  ppm (t, 9H, P- $\text{CH}_3$ ), 0.80–0.85 ppm (w, 6H, P- $\text{CH}_2$ ), 0.97–1.10 (w, 6H,  $\text{CH}_2$ ), 2.50 ppm (s, 6H,  $\text{CH}_3$ ), 3.91 ppm (s, 4H,  $\text{CH}_2\text{CH}_2$ ), 5.74 ppm (s, 2H, CH).

$[\text{Co}(\text{BFE})(\text{PPh}_3)]\text{ClO}_4 \cdot \text{H}_2\text{O}$ ,  $\text{C}_{30}\text{H}_{29}\text{CoClF}_6\text{N}_2\text{O}_7\text{P}$  (768.88), yield: 70%. Calcd: C 46.86, H 3.8, N 3.64. Exp.: C 47.10, H 3.82, N 3.75.  $^1\text{H}$  NMR (250 MHz,  $\text{DMSO-d}_6$ , room temperature, TMS):  $\delta = 2.48$  ppm (s, 6H,  $\text{CH}_3$ ), 3.60 ppm (w, 4H,  $\text{CH}_2\text{CH}_2$ ), 5.23 ppm (s, 2H, CH), 7.21–7.65 ppm (m, 15H, Ar).

$[\text{Co}(\text{BCE})(\text{PBu}_3)]\text{ClO}_4 \cdot \text{H}_2\text{O}$ ,  $\text{C}_{24}\text{H}_{45}\text{CoCl}_3\text{N}_2\text{O}_7\text{P}$  (640.7), yield: 65%. Calcd: C 43.16, H 6.79, N 4.20. Exp.: C 43.68, H 6.83, N 4.24.  $^1\text{H}$  NMR (250 MHz,  $\text{DMSO-d}_6$ , room temperature, TMS):  $\delta = 0.81$ –87 ppm (t, 9H, P- $\text{CH}_3$ ), 1.30–1.41 ppm (w, 18H, P- $\text{CH}_2$ ), 2.10 (s, 6H,  $\text{CH}_3$ ), 2.40 ppm (s, 6H,  $\text{CH}_3$ ), 3.70 ppm (s, 4H,  $\text{CH}_2\text{CH}_2$ ).

### 2.3. Electrochemical measurements

Cyclic voltammograms were performed using an autolab modular electrochemical system (ECO Chemie, Utrecht, The Netherlands) equipped with a PSTA 20 module and driven by GPES (ECO Chemie) in conjunction with a three-electrode system and a personal computer for data storage and processing. A Ag/AgCl (saturated KCl)/3 M KCl reference electrode, a Pt wire as counter electrode and a glassy carbon electrode as working electrode were employed for the electrochemical studies. Voltammetric measurements were performed at room temperature under argon in DMF solution with 0.1 M tetrabutylammonium perchlorate as the supporting electrolyte.

## 3. Results and discussion

### 3.1. IR spectra

The IR spectra of all Schiff bases and their complexes have several prominent bands (tables 1 and 2). A keto amine structure (figure 1) for Schiff-base ligands derived from diketones and diamines were proposed and show that the hydrogen is bonded to both oxygen and nitrogen (NH/OH) [20–23]. The vibrational band of (NH/OH) is observed in the range 3070–3200  $\text{cm}^{-1}$  and disappeared in the spectra of the complexes. The strong band at 1600  $\text{cm}^{-1}$  can be related to C=N and/or C=O bonds [20].

The IR spectra of the complexes show a strong band at 1568–1619  $\text{cm}^{-1}$  due to  $\nu(\text{C}=\text{N})$  [14, 19]. The  $\nu(\text{C}=\text{C})$  appeared in the range 1452–1534  $\text{cm}^{-1}$ . While the Cl functional group shifted the  $\nu(\text{C}=\text{N})$  and  $\nu(\text{C}=\text{C})$  stretching to lower frequency, the  $\text{CF}_3$  functional group shows a reverse effect and vibrational energy of (C=N) and (C=C) is higher. A band due to  $\text{ClO}_4^-$  is around 1089–1140  $\text{cm}^{-1}$  [24]. The peaks about 2960  $\text{cm}^{-1}$  and 3100  $\text{cm}^{-1}$  indicate that  $\text{PR}_3$  coordinates to Co(III). The vibrational

Table 1. IR characterization of the Schiff-base ligands.

No.	Schiff base	OH/NH ( $\text{cm}^{-1}$ )	C–H ( $\text{cm}^{-1}$ )	C=N/C=O ( $\text{cm}^{-1}$ )	C=C ( $\text{cm}^{-1}$ )
1	BAE	3170	3000	1610	1563
2	BCE	3145	3000	1592	1557
3	BBE	3075	2905	1600	1539
4	BFE	3175	3010	1615	1578

Table 2. IR characterization of  $[\text{Co}(\text{Chel})(\text{PR}_3)]\text{ClO}_4 \cdot \text{H}_2\text{O}$  complexes.

No.	Chel	$\text{H}_2\text{O}$	$\text{PBu}_3$	$\text{PPh}_3$	C=N ( $\text{cm}^{-1}$ )	C=C ( $\text{cm}^{-1}$ )	$\text{ClO}_4$ ( $\text{cm}^{-1}$ )
1	BAE	3415	2955	–	1589	1508	1097
2	BAE	3455	–	3110	1586	1507	1088
3	BCE	3430	2965	–	1568	1452	1102
4	BBE	3425	2955	–	1591	1507	1089
5	BBE	3435	–	3070	1592	1505	1089
6	BFE	3430	2970	–	1615	1528	1117
7	BFE	3405	–	3120	1619	1534	1105

peak of H<sub>2</sub>O is in the range 3400–3450 cm<sup>-1</sup>. The absence of coordinated water in the complexes was confirmed by the absence of an absorption at 3100 cm<sup>-1</sup> [25].

### 3.2. Electronic spectra

The electronic spectra of the Schiff bases and their complexes were measured in ethanol and acetonitrile and the results collected in tables 3–6. The electronic spectrum of BAE shows an intense band with maxima at 305 nm and 323 nm ( $\epsilon = 3500 \text{ M}^{-1} \text{ cm}^{-1}$ ) [14]. The splitting in the system has been attributed to coupling of the two azomethines.

Table 3. UV-vis bands of the Schiff-base ligands in EtOH.

No.	Schiff base	$\lambda_{\text{nm}} (\epsilon \text{M}^{-1} \text{cm}^{-1})$			
1	BAE	323(36034)	305(32896)	–	
2	BCE	342(26539)	323(26065)	203(23653)	
3	BBE	348(43754)	245(19456)	204(16993)	
4	BF E	332(30465)	323(30828)	310(29019)	

Table 4. UV-vis bands of the Schiff-base ligands in CH<sub>3</sub>CN.

No.	Schiff base	$\lambda_{\text{nm}} (\epsilon \text{M}^{-1} \text{cm}^{-1})$			
1	BAE	313(36617)	300(36598)	–	–
2	BAC	338(27147)	322(26971)	226(13088)	208(12882)
3	BBE	348(40584)	242(24342)	204(16993)	–
4	BF E	332(29545)	323(29689)	310(29689)	–

Table 5. UV-vis bands of [Co(Chel)(PR<sub>3</sub>)]ClO<sub>4</sub> · H<sub>2</sub>O complexes in EtOH.

No.	Chel	PR <sub>3</sub>	$\lambda_{\text{nm}} (\epsilon \text{M}^{-1} \text{cm}^{-1})$			
1	BAE	PBu <sub>3</sub>	650(367)	422 <sub>sh</sub> (776)	355(5019)	–
2	BBE	PBu <sub>3</sub>	652(500)	–	392(11188)	322(18243)
3	BCE	PBu <sub>3</sub>	661(295)	453 <sub>sh</sub> (481)	373(3415)	–
4	BF E	PBu <sub>3</sub>	611(348)	488(333)	359(4173)	–
5	BAE	PPh <sub>3</sub>	758(196)	454(669)	352 <sub>sh</sub> (5860)	310 <sub>sh</sub> (11462)
6	BBE	PPh <sub>3</sub>	754(215)	–	382(8724)	320(16749)
7	BF E	PPh <sub>3</sub>	691(207)	444(1183)	332(12888)	–

Table 6. UV-vis bands of [Co(Chel)(PR<sub>3</sub>)]ClO<sub>4</sub> · H<sub>2</sub>O complexes in CH<sub>3</sub>CN.

No.	Chel	PR <sub>3</sub>	$\lambda_{\text{nm}} (\epsilon \text{M}^{-1} \text{cm}^{-1})$			
1	BAE	PBu <sub>3</sub>	649(202)	423 <sub>sh</sub> (839)	355(5577)	–
2	BBE	PBu <sub>3</sub>	652(229)	–	389(10139)	318(14522)
3	BCE	PBu <sub>3</sub>	659(212)	455 <sub>sh</sub> (540)	368(3806)	–
4	BF E	PBu <sub>3</sub>	599(274)	499 <sub>sh</sub> (370)	357 (4707)	–
5	BAE	PPh <sub>3</sub>	751(122)	470(835)	356 <sub>sh</sub> (7150)	302(14192)
6	BBE	PPh <sub>3</sub>	748(115)	–	376(9384)	321(16643)
7	BF E	PPh <sub>3</sub>	680(166)	457(1596)	334(14551)	–

In BBE, absorption bands are observed at 350 nm ( $\epsilon = 4000 \text{ M}^{-1} \text{ cm}^{-1}$ ) and 243 nm ( $\epsilon = 20,000 \text{ M}^{-1} \text{ cm}^{-1}$ ). The bands at lower energy are attributable to the  $\pi-\pi^*$  transition assisted by azomethine, and the band at higher energy arises from  $\pi-\pi^*$  transitions within the phenyl rings. The absorption spectrum of BFE shows three absorptions at 310 nm, 323 nm and 332 nm ( $\epsilon = 3000 \text{ M}^{-1} \text{ cm}^{-1}$ ).

After complexation, the Co(III) BAE complexes show absorption bands red-shifted approximately 40–50 nm relative to those of their respective uncomplexed ligands [14].

In the near UV-visible region for the complexes in ethanol and acetonitrile solution there is a band between 330–400 nm ( $\epsilon = 4000\text{--}12,000 \text{ M}^{-1} \text{ cm}^{-1}$ ) attributable to a  $\pi-\pi^*$  interligand transition. In each complex, the band is red-shifted about 40 nm from the corresponding absorption in the free ligand [14]. The solvent has no effect on this transition. Also this band is constant in equilibrium reactions between five-coordinate complexes with different donors [19, 26].

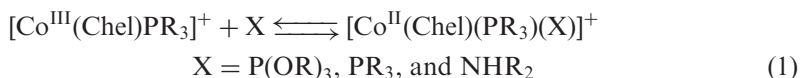
Two bands are observed in the visible region.  $[\text{Co}(\text{Chel})(\text{PR}_3)]^+$  complexes are green and exhibit a low energy transition in the 600–760 nm ( $\epsilon = 200\text{--}400 \text{ M}^{-1} \text{ cm}^{-1}$ ) region of the spectra of Co(III) Schiff-base complexes, as previously reported [18, 27, 28]. This band is affected by the axial and equatorial ligands and the solvent. This transition has been interpreted as being characteristic of five-coordinate, square pyramidal complex and assigned to the d–d transition [18, 28, 29]. For an individual Schiff-base ligand this transition changed about 80–100 nm for different axial ligands (tables 5 and 6). For example the  $\lambda_{\text{max}}$  for  $[\text{Co}(\text{BAE})(\text{PBU}_3)]^+$  is about 650 nm, whereas the  $[\text{Co}(\text{BAE})(\text{PPh}_3)]^+$  complex shows this transition in the range 750–760 nm. In the presence of monodentate axial ligands, the green solution of  $[\text{Co}(\text{Chel})(\text{PR}_3)]^+$  changes to deep red, and the low energy transition is replaced by more intensive absorptions in the range 410–450 nm [15, 16, 18, 19, 26, 27], due to formation of six-coordinate complexes in the presence of axial ligands. Electronic effects of phosphines have been expressed by  $\sigma^*$  values of Taft (Taft constants);  $\sigma^*$  values for  $\text{PPh}_3$  and  $\text{PBU}_3$  are +1.800 and  $-0.390$ , respectively [30, 31]. Axial phosphine ligands have an important steric factor; the cone angles for  $\text{PPh}_3$  and  $\text{PBU}_3$  are 145 and 132, respectively [32]. The transition energy of this band decreases in the trend,  $\text{PBU}_3 > \text{PPh}_3$ . Steric and electronic factors may contribute to the ligand field strengths of  $\text{PR}_3$ , higher for  $\text{PBU}_3$  than  $\text{PPh}_3$  [18]. By increasing the ligand field strength of the axial ligand in five-coordinate complexes  $[\text{Co}(\text{Chel})(\text{PR}_3)]^+$  and also in six-coordinate  $[\text{Co}(\text{Chel})(\text{PR}_3)_2]^+$  complexes, the antibonding character of  $dz^2$  increases;  $dz^2$  is the LUMO in this transition [15, 16].

The electronic effect of equatorial Schiff-base ligand on the electronic spectra of Co(III) complexes is increased in the order  $\text{BFE} > \text{BAE} \approx \text{BBE} > \text{BCE}$  (table 1). The BFE Schiff-base ligand is a weak  $\sigma$ -donor because of the  $\text{CF}_3$  withdrawing group while it is a better  $\pi$  acceptor (see the electrochemical results). The  $\pi$ -interactions between metal d orbitals and  $\pi^*$  orbitals on the Schiff-base ligands increase by increasing  $\pi$  acceptor character ligands. This interaction decreases the energy level of the d orbitals, while energy of the ligand  $\pi^*$  orbitals increases [15, 16, 29]. Therefore the energy of d orbitals decreases via  $\pi$ -interaction with  $\pi^*$  orbitals of BFE ligand and transition energy between d orbitals increases.

The 400–500 nm band is affected by axial and equatorial ligands, but there is not a trend for this effect. The solvent affects this transition in a reverse trend relative to the above d–d transition. The 600–760 nm band shows a blue shift in acetonitrile, while the 400–500 nm transition is red-shifted in acetonitrile relative to the ethanol.

### 3.3. Coordination number of the studied complexes

Although [Co(III)(DH)<sub>2</sub>] (DH = dimethylglyoximate) complexes appear to be invariably six-coordinate, five-coordinate complexes of the type [(Co(Chel)X)] (where Chel = Salen, Salopen, BAE and their derivatives) are formed when X is a highly polarizable, strong  $\sigma$  donor such as an alkyl group or a tertiary phosphine [24, 29]. Many axial ligand equilibrium studies are available [18–19, 26–28, 34–37]; although the equilibrium constants for the reaction are decreased with increasing the donor number of solvent [26, 34–36].



From the results it seems that the H<sub>2</sub>O molecule is weakly bonded to this type of complex and replaced by donor solvents or by other ligands like phosphines, phosphites and amines.

### 3.4. The electrochemical properties of cobalt Schiff-base complexes

A typical cyclic voltammogram of [Co(BAE)(PBu<sub>3</sub>)]<sup>+</sup> in the potential range +0.2 to –2 V (vs. Ag/AgCl) in DMF solution is shown in figure 2(a). A first reduction peak is observed about –0.479 V due to:

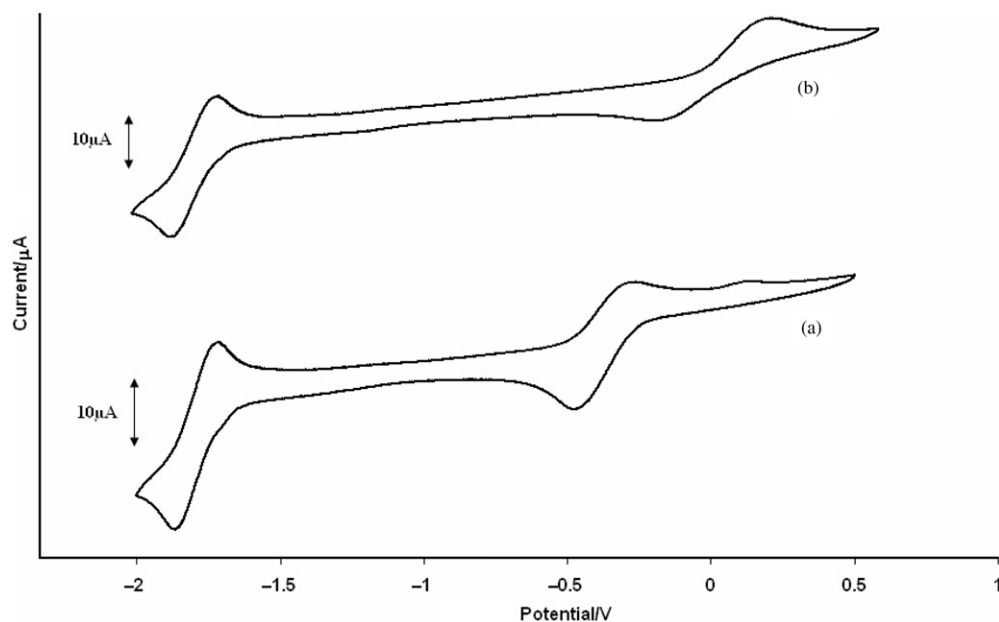
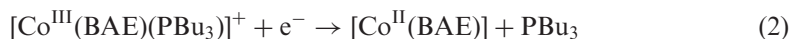


Figure 2. Cyclic voltammogram of [Co(BAE)(PR<sub>3</sub>)]ClO<sub>4</sub> · H<sub>2</sub>O, (a) (R = Bu), (b) (R = Ph), in DMF at room temperature. Scan rate: 100 mV s<sup>-1</sup>.



Table 7. Reduction potentials (V) for [Co(Chel)(PR<sub>3</sub>)ClO<sub>4</sub>·H<sub>2</sub>O] complexes in DMF.

No.	Chel	PR <sub>3</sub>	$E_{pa}(II \rightarrow III)$	$E_{pc}(III \rightarrow II)$	$E_{1/2}(II \leftrightarrow I)$
1	BAE	PBu <sub>3</sub>	-0.274(0.116)	-0.479	-1.790
2	BAE	PBu <sub>3</sub> (excess)	-0.313	-0.498	-1.790
3	BAE	PPh <sub>3</sub>	0.136	-0.225	-1.795
4	BAE	PPu <sub>3</sub> (excess)	0.009	-0.225	-1.795
5	BBE	PBu <sub>3</sub>	-0.254(0.174)	-0.440	-1.605
6	BBE	PBu <sub>3</sub> (excess)	-0.293	-0.488	-1.605
7	BBE	PPh <sub>3</sub>	0.165	-0.176	-1.644
8	BBE	PPu <sub>3</sub> (excess)	0.048	0.048	-1.634
9	BCE	PBu <sub>3</sub>	-0.229(0.175)	-0.367	-1.5
10	BCE	PBu <sub>3</sub> (excess)	-0.325	-0.473	-1.5
11	BFE	PBu <sub>3</sub>	-0.181(0.202)	-0.377	-1.298
12	BFE	PBu <sub>3</sub> (excess)	-0.207	-0.394	-1.298
13	BFE	PPh <sub>3</sub>	0.271	-0.074	-1.267
14	BFE	PPu <sub>3</sub> (excess)	0.094	-0.092	-1.280

The electron is added to the antibonding  $dz^2$  orbital and the product Co(II) complex loses its axial ligand in weakly coordinating solvents [14–16]. The second quasi-reversible process at ca  $-1.790$  V is observed with about unit ratio of anodic to cathodic peak currents ( $i_{pa}/i_{pc}$ ), corresponding to the simple one-electron process:



Upon reversal of the scan direction, the Co(II) complex is oxidized to Co(III) at higher potentials (about 200 mV). Then, in a rapid consecutive reaction, the five-coordinate  $[Co^{III}(BAE)(PR_3)]^+$  is formed again (i.e., the electron transfer is followed by a chemical reaction) [14–16]. Multiple scans resulted in nearly superimposable cyclic voltammograms, thereby showing marked stability of the three oxidation states of cobalt involved in the electrochemical study. The reduction and oxidation potentials for the different complexes are presented in table 7.

The formal potentials for the reversible Co(II/I) redox couple were calculated as the average of the cathodic ( $E_{pc}$ ) and anodic ( $E_{pa}$ ) peak potentials of this process. The effect of phosphine as axial ligand and equatorial Schiff-base ligand on the electrochemical behavior of Co(III) Schiff-base complexes are described below.

### 3.5. The effect of the axial ligand on electrochemical properties of Co complexes

The observed cathodic peak potentials  $E_{pc}$  for the reduction  $Co(III) + e^- \rightarrow Co(II)$  strongly depend on the  $\sigma$ -donor strength of the phosphine axial ligand [14–16, 18]. The  $\sigma$ -donor strength of the different axial ligands is also reflected in the spectra of the complexes. The energy of the transition between 600–760 nm decreases in the order  $PBu_3 > PPh_3$ . Similar trends are observed for the reduction of Co(III) to Co(II) and oxidation of Co(II) to Co(III). The BAE complex involving  $PBu_3$  as axial ligand is reduced at  $-0.479$  V, whereas the reduction wave for  $PPh_3$  as axial ligand anodically shifts to  $-0.222$  V (table 7 and figure 2b).

The oxidation of the  $Co(II) \rightarrow Co(III)$  also depends on the type and concentration of axial ligand. In general for  $[Co(Chel)(PBu_3)]^+$  two peaks appear for oxidation of Co(II) (figure 3a and table 7). The following two reactions are responsible for this

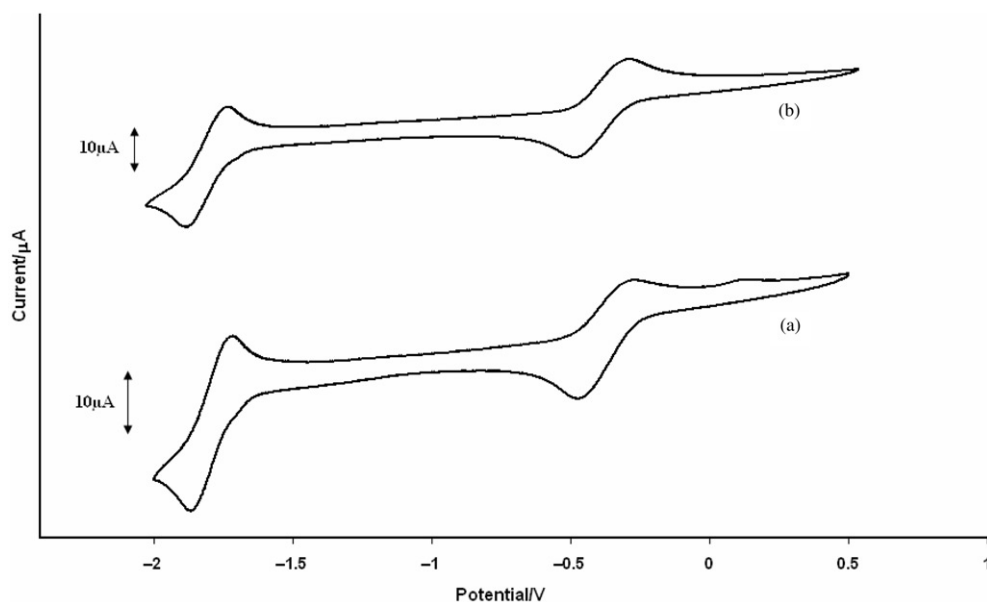
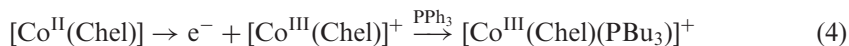


Figure 3. Cyclic voltammogram of (a)  $[\text{Co}(\text{BAE})(\text{PBu}_3)]\text{ClO}_4 \cdot \text{H}_2\text{O}$ , (b) (0.001 M,  $\text{PBu}_3$ ) in DMF at room temperature. Scan rate:  $100 \text{ mV s}^{-1}$ .

observation:



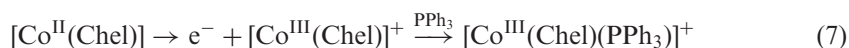
Oxidation happens at higher potentials and also depends on the equatorial ligand (table 7) while  $[\text{Co}(\text{Chel})(\text{PBu}_3)]$  is oxidized at lower potentials. At low scan rates the concentration of  $[\text{Co}^{\text{II}}(\text{Chel})(\text{PBu}_3)]$  is important and the current is higher at lower potentials (reaction 5). By increasing the scan rate, reaction 4 is more important and the peak at positive potentials has a high current.

Figure 3(b) shows the effect of  $\text{PR}_3$  concentration on the electrochemical behaviour of  $[\text{Co}^{\text{III}}(\text{BAE})(\text{PR}_3)]^+$ . Upon addition of phosphine (0.001 M), both peaks disappear and oxidation occurs at lower potential and the reduction wave shifts in the negative direction (six-coordinate complex is formed). In the presence of phosphine the following reaction occurs:



The changes are due to increasing the antibonding character of the  $\text{d}_{z^2}$  orbital via addition of  $\text{PR}_3$ . In contrast, the  $\text{Co}(\text{II}/\text{I})$  couple is not affected by concentration of phosphine.

$\text{PPh}_3$  as axial ligand has a large cone angle and low  $\sigma$ -donor strength so there is only one peak for oxidation of the  $\text{Co}(\text{II}) \rightarrow \text{Co}(\text{III})$  that arises from the following reaction:



At high concentration of  $\text{PPh}_3$  this peak shifts to lower potentials that according to the following reaction arises from oxidation of  $[\text{Co}^{\text{II}}(\text{Chel})(\text{PPh}_3)]$ .



### 3.6. The effect of the equatorial ligand on electrochemical properties of Co complexes

Equatorial ligand substitutions generally affect reduction potentials less than the axial ligands, consistent with electron transfer to  $\text{d}z^2$  by formation of  $\text{Co}(\text{II})$ . Functional groups like  $\text{CF}_3$ ,  $\text{Cl}$  and  $\text{Ph}$  on the Schiff base lead to an anodic shift of peak potentials ( $E_{\text{pc}}$ ) for complexes with the same axial ligand, thus making the BAE substituted complexes easier to reduce (table 7 and figure 4). The reason for this is electron-withdrawing character of the substituents, which decrease the electron density on the metal [14].

The  $\text{Co}^{\text{(II/I)}}(\text{BAE})$  couples are not influenced by potential axial ligands, which indicates that only four-coordinate species are involved in the electrode reactions. Equatorial substituents affect these potentials in the same way as for  $\text{Co}(\text{III/II})$  couples. However, while the maximum range of  $\text{Co}(\text{III/II})$  potentials is only 100 mV (for constant axial ligand), the range of the corresponding  $\text{Co}(\text{II/I})$  couples are about 492 mV. The greater dependence of the  $\text{Co}(\text{II/I})$  couple on the nature of the equatorial ligand is due to the lower oxidation states that are better electron donors to the  $\pi^*$  orbitals of Schiff base [14–16]. From the  $\text{Co}(\text{II/I})$  couples, the  $\pi$ -acceptor property of the BAE Schiff-base derivatives is in the following trend:

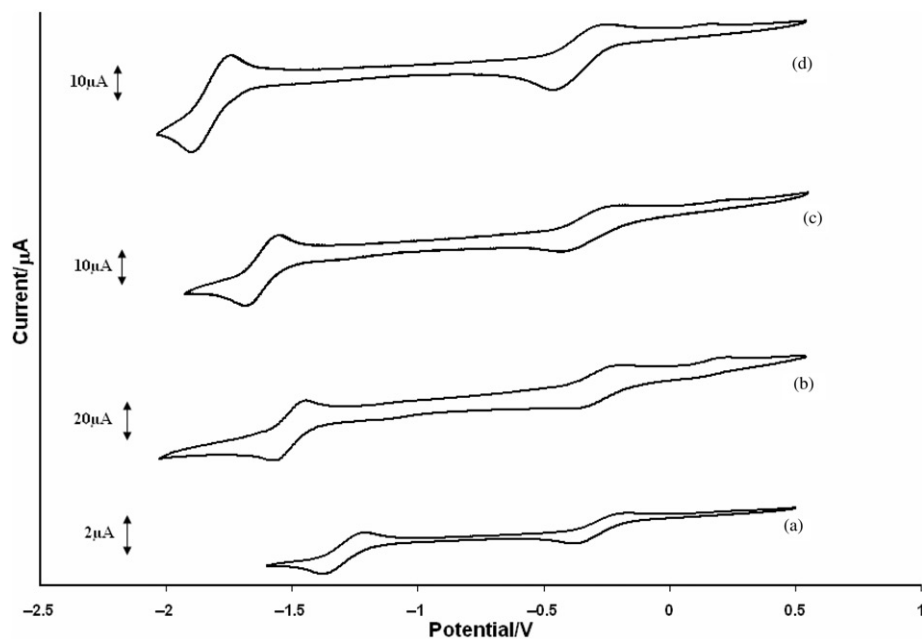
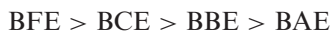
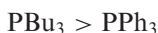


Figure 4. Cyclic voltammograms of  $[\text{Co}(\text{Chel})(\text{PBu}_3)]\text{ClO}_4 \cdot \text{H}_2\text{O}$ , ( $\text{Chel} =$  (a) (BFE), (b) (BCE), (c) (BBE), (d) (BAE)).

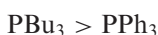
#### 4. Conclusions

By considering the UV-vis spectroscopy and electrochemical behavior of pentacoordinate Co(III) Schiff-base complexes, the following conclusions have been drawn:

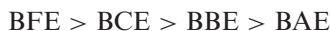
- (1) The ligand field strength of pentacoordinate Co(III) Schiff-base complexes like  $[\text{Co}(\text{Chel})(\text{PR}_3)]\text{ClO}_4 \cdot \text{H}_2\text{O}$  is arranged according to the following trend for phosphine axial ligands:



- (2) The cathodic peak potentials  $E_{\text{pc}}$  for the reduction  $\text{Co(III)} + e^- \rightarrow \text{Co(II)}$  depend on the nature of the axial ligand in the order:



- (3) The  $\text{Co}^{(\text{II/I})}$ (BAE) couples are not influenced by potential axial ligands.  
 (4) From the reduction potentials the  $\pi$ -acceptor property of the BAE derivatives is arranged in the trend:



#### References

- [1] L. Canali, D.C. Sherrington. *Chem. Soc. Rev.*, **28**, 85 (1998).
- [2] A.A. Isse, A. Gennaro, E. Vianello. *J. Electroanal. Chem.*, **444**, 241 (1998).
- [3] D. Pletcher, H. Thompson. *J. Electroanal. Chem.*, **464**, 168 (1999).
- [4] T. Okada, K. Katou, T. Hirose, M. Yuasa, I. Sekine. *J. Electrochem. Soc.*, **146**, 2562 (1999).
- [5] P.H. Aubert, A. Neudeck, L. Dunsch, P. Audebert, P. Capdevielle, M. Maumy. *J. Electroanal. Chem.*, **481**, 24 (2000).
- [6] L. Mao, K. Yamamoto, W. Zhou, L. Jin. *Electroanalysis*, **12**, 72 (2000).
- [7] E.G. Jäger, K. Schuhmann, H. Görls. *Inorg. Chim. Acta*, **255**, 295 (1997).
- [8] E. Eichhorn, A. Rieker, B. Speiser. *Angew. Chem., Int. Ed. Engl.*, **31**, 1215 (1992).
- [9] E. Eichhorn, A. Rieker, B. Speiser, J. Sieglén, J. Strahle. *Z. Naturforsch.*, **48b**, 418 (1993).
- [10] E. Eichhorn, A. Rieker, B. Speiser, H. Stahl. *Inorg. Chem.*, **36**, 3307 (1997).
- [11] E. Eichhorn, B. Speiser. *J. Electroanal. Chem. Interfacial Electrochem.*, **365**, 207 (1994).
- [12] B. Speiser, H. Stahl. *Angew. Chem. Int. Ed. Engl.*, **34**, 1086 (1995).
- [13] B. Golles, B. Speiser, H. Stahl, J. Sieglén, J. Strahle. *Z. Naturforsch.*, **51b**, 388 (1996).
- [14] A. Botcher, T. Takeuchi, I. Hardcastle, T.J. Mead, H.B. Gray, D. Cwikel, M. Kapon. *Z. Dori. Inorg. Chem.*, **36**, 2498 (1997).
- [15] A.H. Sarvestani, A. Salimi, S. Mohebbi, R. Hallaj. *J. Chem. Res.*, 190 (2005).
- [16] A.H. Sarvestani, S. Mohebbi. *J. Chem. Res.*, 257 (2006).
- [17] P.J. McCarthy, R.J. Hover, K. Uexo, A.E. Martelo. *J. Am. Chem. Soc.*, **77**, 5820 (1955).
- [18] C.W. Smith, G.W. Van Loon, M.C. Barid. *Can. J. Chem.*, **54**, 1875 (1976).
- [19] M. Asadi, A.H. Sarvestani, Z. Asadi, M. Setoodekhah. *Syn. React. Inorg. Metal-Org. Nano-Metal Chem.*, **35**, 639 (2005).
- [20] Ch. Yu-Ying, E.Ch. Doris, B.D. McKinney, L.J. Willis, S.C. Cumming. *Inorg. Chem.*, **20**, 1885 (1981).
- [21] E. Kwiatkowski, M. Kwiatkowski. *Inorg. Chim. Acta*, **82**, 101 (1984).
- [22] J.P. Costes, M.I. Fernandes-Garcia. *Inorg. Chim. Acta*, **237**, 57 (1995).
- [23] A.D. Garnovskii, A.L. Nivorozhkin, V.I. Minkin. *Coord. Chem. Rev.*, **126**, 1 (1993).
- [24] B. Adhikary, K. Mitra, S. Biswas, C.R. Lucas. *Inorg. Chim. Acta*, **359**, 1997 (2006).
- [25] S.M. Polson, R. Cini, C. Pfferi, L.G. Marzilli. *Inorg. Chem.*, **36**, 314 (1997).
- [26] M. Asadi, A.H. Sarvestani, M.B. Ahmadi, Kh. Mohammadi, Z. Asadi. *J. Chem. Thermodyn.*, **36**, 141 (2004).
- [27] M. Asadi, A.H. Sarvestani. *Can. J. Chem.*, **79**, 1360 (2001).
- [28] G. Tazdher, G. Mestroni, A. Puxeddu, R. Costanzo, G. Costa. *J. Chem. Soc. (A)*, 2504 (1971).

- [29] D.F. Shriver, P.W. Atkins. *Inorganic Chemistry*, p. 240, Oxford University Press, Oxford (1999).
- [30] W.A. Henderson Jr, C.A. Streuli. *J. Am. Chem. Soc.*, **82**, 5791 (1960).
- [31] R.W. Taft Jr. In *Steric Effects in Organic Chemistry*, M.S. Newman (Ed.), p. 619, Wiley, New York (1956).
- [32] T.L. Brown, K.J. Lee. *Coord. Chem. Rev.*, **128**, 89 (1993).
- [33] G. Costa, G. Mestroni, L. Stefani. *J. Organomet. Chem.*, **7**, 493 (1967).
- [34] M. Asadi, A.H. Sarvestani. *J. Chem. Res. (s)*, 520 (2002).
- [35] M. Asadi, Kh. Mohammadi, A.H. Kianfar. *Iranian J. Chem. Soc.*, **3**, 247 (2006).
- [36] A.H. Sarvestani, M. Asadi, M. Abbasi. *J. Chem. Res.*, **56** (2007).
- [37] M. Amirnasr, V. Langer, N. Rasouli, M. Salehi, S. Meghdadi. *Can. J. Chem.*, **83**, 2073 (2005).